JOURNAL OF MATERIALS SCIENCE **37** (2002) 3603–3613

Relationship between stress-induced martensitic transformation and impact toughness in low carbon austenitic steels

M.-X. ZHANG, P. M. KELLY
Department of Mining, Minerals and Materials Engineering, University of Queensland, St. Lucia, Brisbane, QLD 4072, Australia
E-mail: M.Zhang@minmet.uq.edu.au

The effect of test temperature, which controls the stability of austenite, on the impact toughness of a low carbon Fe-Ni-Mn-C austenitic steel and 304 stainless steel, has been investigated. Under impact conditions, stress-induced martensitic transformation occurred, in a region near the fracture surface, at test temperatures below 80°C for the Fe-Ni-Mn-C steel and below −25°C for 304 stainless steel. The former shows significant transformation toughening and the highest impact toughness was obtained at 10°C, which corresponds to the maximum amount of martensite formed by stress-induced transformation above the Ms temperature. The stress-induced martensitic transformation contributes negatively to the impact toughness in the 304 stainless steel. Increasing the amount of stress-induced transformation to martensite, lowered the impact toughness. The experimental results can be well explained by the Antolovich theory through the analysis of metallography and fractography. The different effect of stress-induced transformation on the impact toughness in Fe-Ni-Mn-C steel and 304 stainless steel has been further understood by applying the crystallographic model for stress-induced martensitic transformation to these two steels.

1. Introduction

Toughening associated with the stress-induced martensitic transformation has been used to improve the toughness of a wide range of materials [1] and may be used in a controlled way to design alloys with high strength and high toughness [2]. This has been proved theoretically and experimentally in the last few decades in both ferrous alloys [1–10] and ceramic materials [11–15]. As mentioned in a previous paper [16], there are a number of features of the stress-induced transformation and subsequent transformation toughening that are the same in ferrous alloys and ceramic materials. However, there are also some differences in the transformation toughening of these two classes of materials. In most steels, the martensite is very brittle, while the parent austenite is very tough. But, both the new and the parent phases in ceramics are brittle. Hence, the extend of transformation toughening in these two materials differs. Antolovich [1] has suggested that, since martensite is more susceptible to crack propagation than the parent austenite, the magnitude of the toughness change resulted from the stress-induced martensitic transformation depends on the fracture properties of the new phase and the energy being dissipated during the transformation process. This implies that the stress-induced martensitic transformation may make either a net positive or a net negative contribution to the toughness of steels. Most previous work [1–10] reported an increase of fracture toughness resulting from the transformation. Our recent work [16] has shown that the stress-induced martensitic transformation decreases the impact toughness of high carbon Fe-Ni-C alloy, while the impact toughness of a white cast iron was improved when the stress-induced transformation occurred.

The fracture properties or toughness of martensite in steels depends mainly on the carbon content and on the test temperature. Normally, high carbon martensite has low toughness. When the test temperature is below the impact transition temperature (ITT) of the martensite, low toughness is obtained. In addition, the stability of austenite depends on the test temperature too for given material [9]. If the testing is done at high temperature, the austenite may be too stable to transform, and of course, there is no transformation toughening. If the transformation occurs below the ITT of the transformed product, reduction of toughness is more likely. This leads to the concept that stress-induced transformation that results in positive net transformation toughening must occur above the ITT of the newly formed phase, martensite.

In the present work, three low-carbon steels were examined. One has very stable austenite and there is no stress-induced martensitic transformation within all test temperature range. The other alloy has less stable austenite and the stress-induced transformation can occur at room temperature under impact conditions.

TABLE I Chemical composition of the alloys used in the present work (%wt)

Alloys	C	Cr	Si	Mo	Ni	Cu	Mn
304	<0.03	19.0	<0.2	–	10.0	–	–
5.8Mn	0.126	–	0.676	–	20.9	–	5.82
2.6Mn	0.107	–	0.634	–	19.44	–	2.61

The stress-induced martensitic transformation does not occur in the third alloy (304 stainless steel) until the test temperature is below −25°C.

2. Experimental

One commercial 304 stainless steel and two low carbon Fe-Ni-Mn-C steels have been used in the present work. Their chemical compositions are listed in Table I. The 304 steel was supplied as 25 mm diameter bars. After a homogenising annealing treatment at 1150°C for 24 hours, standard Charpy specimens were machined from the bars. The impact tests were carried out over the temperature range from −196°C to 250°C. The 2.6Mn and 5.8Mn Fe-Ni-Mn-C alloys were melted in an air-induction furnace and cast into 25 × 25 mm square bars. All the cast bars of 5.8Mn alloy and part of cast bars of 2.6Mn alloy were hot rolled down to 15 × 15 mm square bars, given a homogenisation anneal at 1150°C for 48 hours, and then standard Charpy specimens were machined from the bars. The Charpy specimens were then solution treated at 900°C for 1 hour. For the 5.8Mn alloy, after water quenching, the Charpy specimens were fully austenitic at room temperature, and impact tests were carried out over the temperature range from −196°C to +100°C. For the 2.6Mn alloy, because martensite would form if it were cooled down to room temperature (Ms temperature is 80°C), the Charpy specimens were directly transferred to a 130° furnace from solution treatment temperature (900°C) in order to obtain a fully austenitic structure. Then, the impact test was undertaken from −196°C to 310°C using these 130°C Charpy specimens. Other part of 2.6Mn alloy cast bars were rolled in two steps in order to increase the stability of austenite. First, the as cast bars were hot rolled down to 18 × 18 mm, and then reheated to 900°C. Second, the bars were rolled at about 450°C to the size of 15 × 15 mm. After this process, 100% austenite was obtained on cooling to room temperature. Charpy specimens were then machined and impact tests were carried out over the temperature range from −25°C to 300°C. To distinguish these two different processes for 2.6Mn alloy, the former is termed solution treated 2.6Mn and the later is called dual rolled 2.6Mn.

The Ms temperatures of all alloys were estimated by cooling the alloy blocks to various temperatures and checking for ferromagnetism using a hand magnet. Before impact testing, each specimen was checked with a hand magnet to ensure that no ferrite or martensite had formed in the specimens.

To obtain the work of crack propagation for different microstructures, Charpy size specimens with a 1 mm deep notch were pre-cracked a further 1 mm by three-point bend fatigue. The impact energy obtained from these pre-cracked specimens denotes the work of crack propagation.

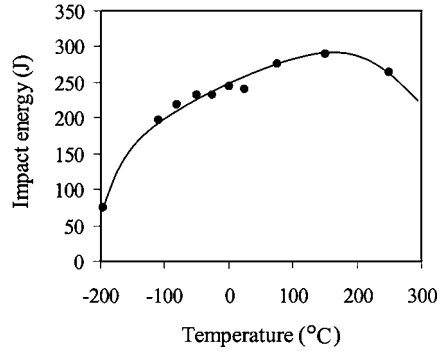

Figure 1 Variation of the Charpy impact energy with test temperature in 304 stainless steel.

The morphology of martensite in 304 stainless steel was revealed by etching with a solution consisting of 0.05×10^{-3} m^3 HCl + 10 gram $CuSO_4 + 0.05 \times 10^{-3}$ m^3 H_2O. The solution used to etch martensite with 2.6Mn alloy was 25% HNO_3 in methanol. The volume fraction of martensite formed during the impact process was measured using a quantitative metallographic method. The fractographic analysis was carried out in a Philips XL30 scanning electron microscopy at voltage of 25 kV. The lattice parameters of austenite and martensite were determined by X-ray diffraction.

3. Results

3.1. Relationship between impact toughness and test temperature

3.1.1. 304 stainless steel

Fig. 1 shows the variation of Charpy impact energy with test temperature. When the temperature is below 150°C, the impact energy decreases with the decrease of the test temperature. When the test temperature falls from −110°C to −196°C, the impact energy is dramatically reduced from 197 J to 74 J. At 250°C the impact energy is slightly lower than that at 150°C. This result is consistent with the impact test results for high carbon Fe-Ni-C alloy [16].

3.1.2. 2.6Mn alloy

The variation of Charpy impact energy with the test temperature of the 2.6Mn alloy in the solution treated condition and the dual rolled condition is shown in Fig.2a and b, respectively. It can be seen that both curves have a similar shape and each curve shows a peak at a certain temperature. For the solution treated 2.6Mn alloy, the peak temperature is 100°C, and for the dual rolled 2.6Mn alloy it is 10°C. When the test temperature is above this peak temperature, the impact energy first drops dramatically and then slowly decreases with increase in the test temperatures. When the test temperature is below the peak temperature, the Charpy impact energy decreases significantly with the decrease in the test temperature. It can also been seen that the high temperature impact toughness is much higher than that at low temperature. These results are consistent with the variation of unnotched impact energy with test temperature for white cast irons [16].

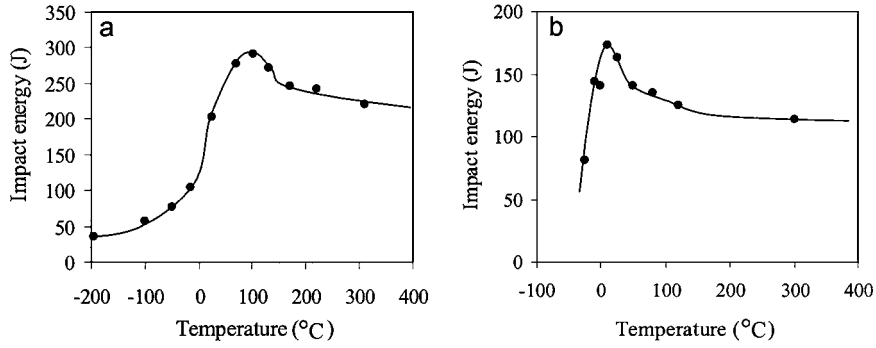

Figure 2 Variation of Charpy impact energy of 2.6Mn alloy with test temperature. (a) solution treatment condition and (b) dual rolled condition.

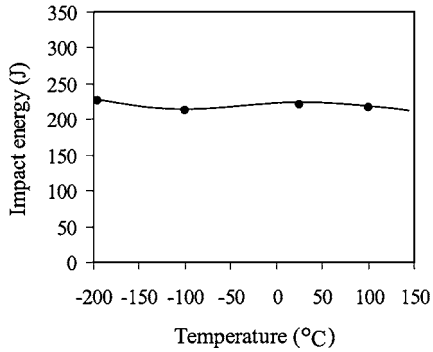

Figure 3 Variation of the Charpy impact energy with test temperature in 5.8Mn alloy.

3.1.3. 5.8Mn alloy

Fig. 3 shows the Charpy impact energy of 5.8Mn alloy at different test temperature. Within the test temperature range of −196°C to 100°C, there was no stress-induced martensitic transformation has been detected using a hand magnet. Fig. 3 shows the impact toughness of pure austenite in the 5.8Mn alloy. Obviously, the impact toughness does not vary significantly with the test temperature. This implies that the test temperature does not affect the impact toughness of austenite over the range of −196°C to 100°C. In addition, it is noted that the impact energy of austenite for 5.8Mn alloy is close to that for solution treated 2.6Mn alloy. But, there is a big difference between 5.8Mn alloy and the dual-rolled 2.6Mn alloy. This is attributed to the high-density dislocations and internal stress generated during the second rolling process in the dual-rolled 2.6Mn alloy.

3.2. Microstructure formed during the impact process

3.2.1. 304 Stainless steel

The Ms temperature of the 304 stainless steel used in the present work has been determined to be below −196°C using the magnetic method described in the experimental section. But, α martensite was detected by a hand magnet on the fracture surface of Charpy specimens, which had been tested at and below −25°C. As the test temperature decreased, the magnetism detected on the fracture surface increased. This implies that the amount of α martensite is increasing. Metallographic analysis has confirmed that a martensitic zone was formed near the fracture surface on both sides of a broken Charpy specimen. Fig. 4 shows the typical martensitic zones near the fracture surface of broken Charpy specimens tested at −196°C, −110°C and −25°C. It can be seen that the size of martensite zones in these different specimens is almost the same. However, the volume fraction of martensite within the martensitic zone increased with the decrease in test temperature.

Fig. 5 shows the microstructure in the martensitic zone at higher magnification for the specimens tested at −196°C, −110°C and −25°C. According to the results of previous work [17, 18] and the present observation in Fig. 5, it can be known that two types of martensite formed within the martensitic zone. One of these is ε martensite, and other is α martensite. Very early work [17, 18] on Fe-Ni-Cr stainless steels has proved the existence of an HCP ε Martensite in cold-worked alloys. The ε martensite is strip-like and the α martensite normally is very fine and forms within the ε martensite [17, 18]. The mixture of α and ε martensite in the martensitic zone can be seen from Fig. 5. The lower the test temperature, the more α martensite is observed.

3.2.2. Dual rolled 2.6Mn alloy

The Ms temperature determined for the 2.6Mn alloy is around 80°C for the solution treatment condition and is approximately 0°C for the dual rolled condition. The decrease of Ms temperature is due to the work hardening of austenite during the second rolling. Hence, martensite has already formed at room temperature in the solution treated 2.6Mn alloy. This makes it the difficult to distinguish the stress-induced martensite from the athermal martensite. The Ms temperature of the dual rolled 2.6Mn alloy is below room temperature and only the stress-induced martensite can be observed at room temperature. Like the 304 stainless steel tested at low temperature, martensitic zone formed near the fracture surface of the broken Charpy specimens in the dual rolled 2.6Mn alloy. Fig. 6a, b and c shows the martensitic zones of the broken Charpy specimens that were tested at 10°C, 25°C and 50°C. When test temperature is at or below 0°C, athermal martensite formed and the stress-induced martensitic zone can not be differentiated. When the test temperature is at or above 80°C, no clear martensitic zone was observed. Unlike 304 stainless steel, the size of the martensitic zone of the dual rolled 2.6Mn alloy varies with the test temperature. The lower the test temperature, the larger the

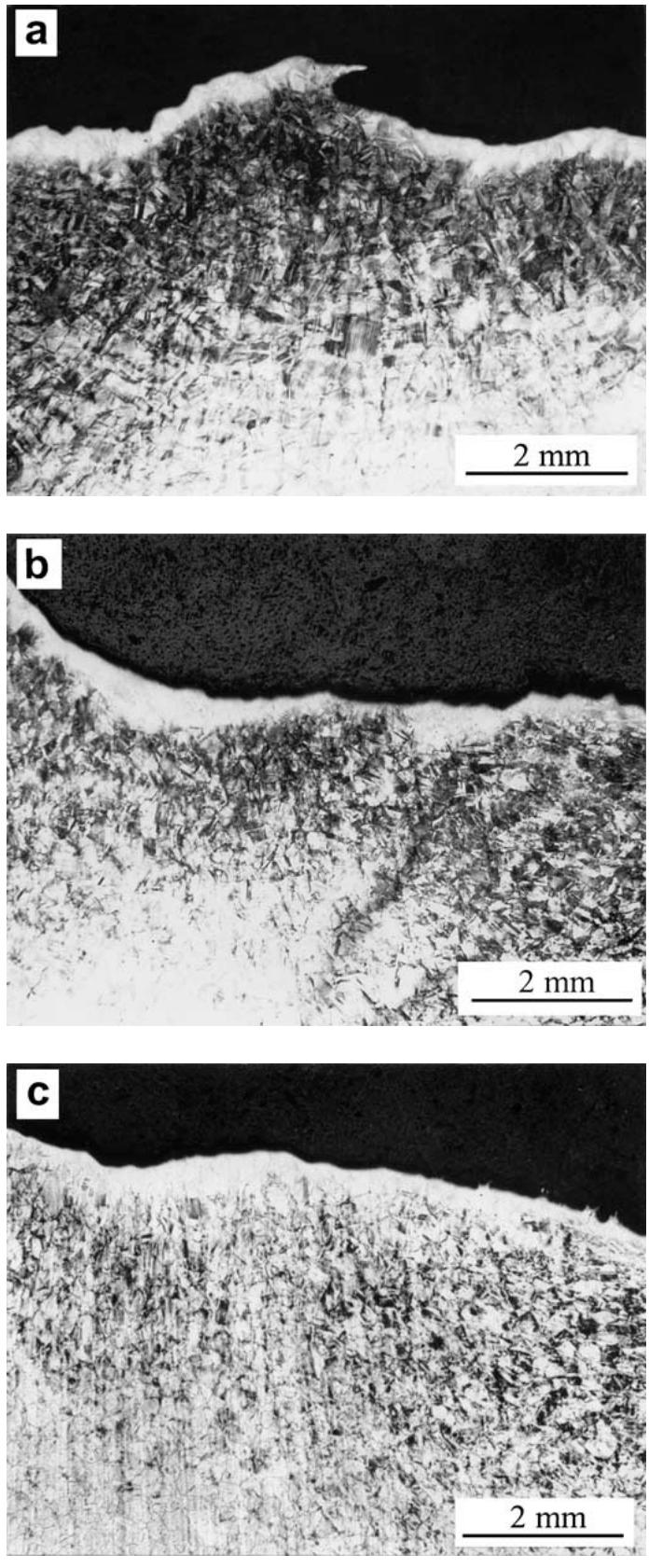

Figure 4 Optical micrographs showing the martensite zone near the fracture surface of Charpy impact specimens that were tested at −196°C, −110°C and −25°C for 304 stainless steel. (a) −196°C, (b) −110°C and (c) −25°C.

martensitic zone. Further analysis of the microstructures within the martensitic zone at higher magnification has shown that only α martensite is formed through the stress-induced transformation in this alloy, as shown in Fig. 6a', b' and c'. There is no ε martensite observed at any test temperature in this alloy.

The volume fraction of martensite within the martensitic zone as determined by quantitative metallography, was 0.20, 0.21 and 0.22 for the specimens tested at 10°C, 25°C and 50°C, respectively. This implies that although the size of the martensitic zone varies significantly with the test temperature, the average volume

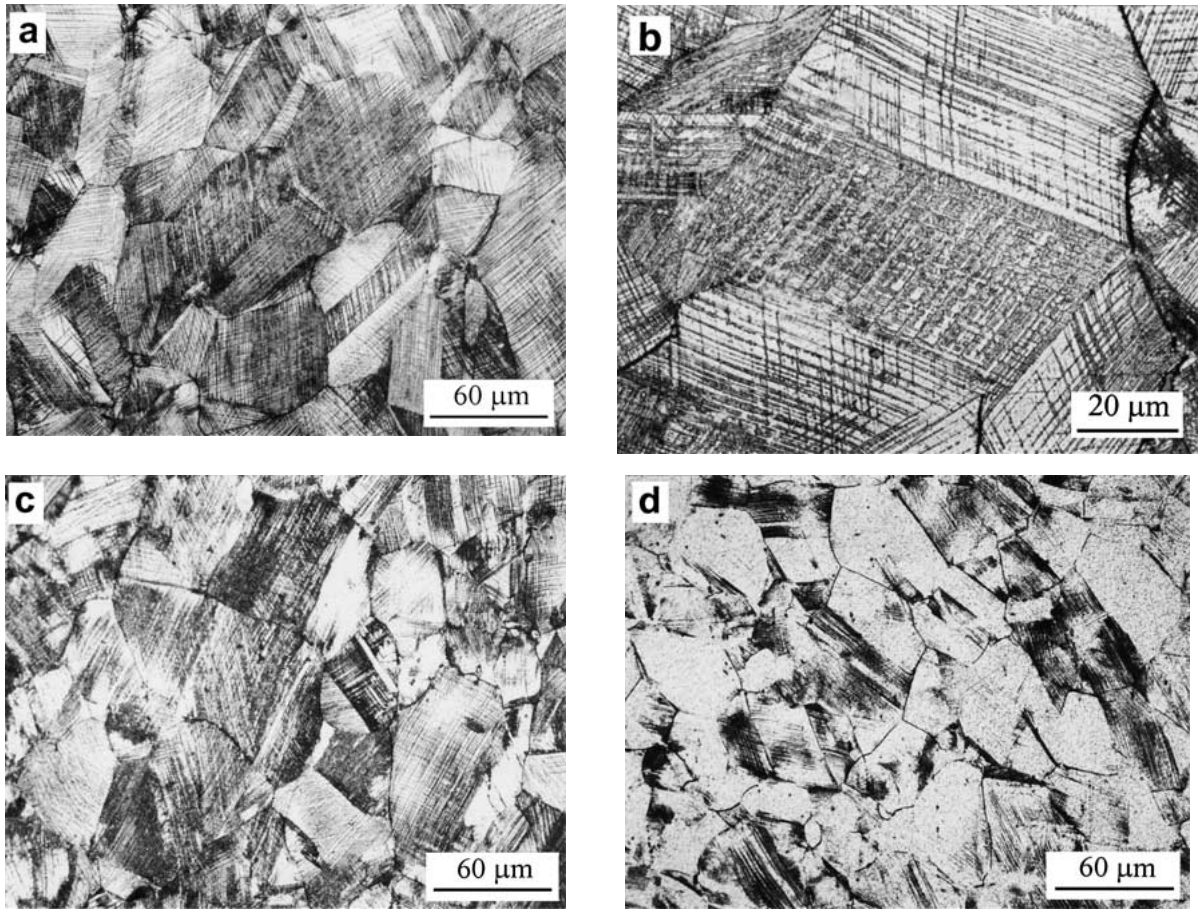

Figure 5 Optical micrographs showing the mixture of α and ε martensite within the martensitic zone under higher magnification for 304 stainless steel specimens tested at different temperature. (a, b) −196°C, (c) −110°C and (d) −25°C.

fraction of martensite within the martensitic zone is not sensitive to the test temperature. This is different from the observation of a high carbon Fe-Ni-C alloy [16] and the 304 stainless steel used in the present work.

3.3. Fractography of 304 stainless steel and the dual rolled 2.6Mn alloy

3.3.1. 304 Stainless steel

Fig. 7 shows the fracture surfaces of the 304 stainless steel Charpy specimens impacted at different temperature. Fig. 7a and b for 75°C and 25°C shows typical large dimples, which are fracture characterisations of the ductile austenite. Fig. 7c, for −110°C where stress-induced martensitic transformation occurred during impacting, shows the mixture of dimples and cleavages. The dimples correspond to the fracture of austenite, and the cleavage is typical fracture characteristics of martensite. Decreasing test temperature resulted in more stress-induced martensite forming in 304 stainless steel. More cleavage fracture occurred in the Charpy specimen. Fig. 7d for −196°C shows more cleavage fracture surface.

3.3.2. The dual rolled 2.6Mn alloy

The fracture surface of impact specimens of the dual rolled 2.6Mn alloy is shown in Fig. 8. The fractography of Charpy specimen impacted at 300°C is the typical dimples as shown in Fig. 8a. Impact testing at 50°C results in a formation of stress-induced martensite near the fracture surface of Charpy specimens as shown in Fig. 6c and c'. Thus, the fracture surface shows the mixture of dimples and quasi-cleavage, which is the fracture characteristic in between ductile fracture and brittle fracture. Decreasing impact test temperature to 10°C results in more stress-induced martensite formed near the fracture surface, and therefore the fractography shows more quasi-cleavage as shown in Fig. 8c. Fig. 8d, for −25°C where the test temperature is below Ms temperature athermal martensite formed before impacting, still shows quasi-cleavage, occasionally with some dimples. From this fractographic analysis it can be seen that martensite in 2.6Mn alloy is more ductile than the martensite in 304 stainless steel and in the high carbon Fe-Ni-C alloy [16]. Hence, formation of stress-induced martensite at Charpy impact conditions leads to the improvement of impact toughness.

4. Discussion

4.1. General discussion

From Figs 7 and 8 it can be seen that the fractography of both 304 stainless steel and the dual rolled 2.6Mn alloy consists of cleavage/quasi-cleavage and dimples for the specimens, in which the stress-induced martensitic transformation occurred. The cleavage/quasi-cleavage corresponds to the fracture in the martensite and the dimples correspond to fracture in the retained austenite. Hence, the formation of martensite at the tip of the

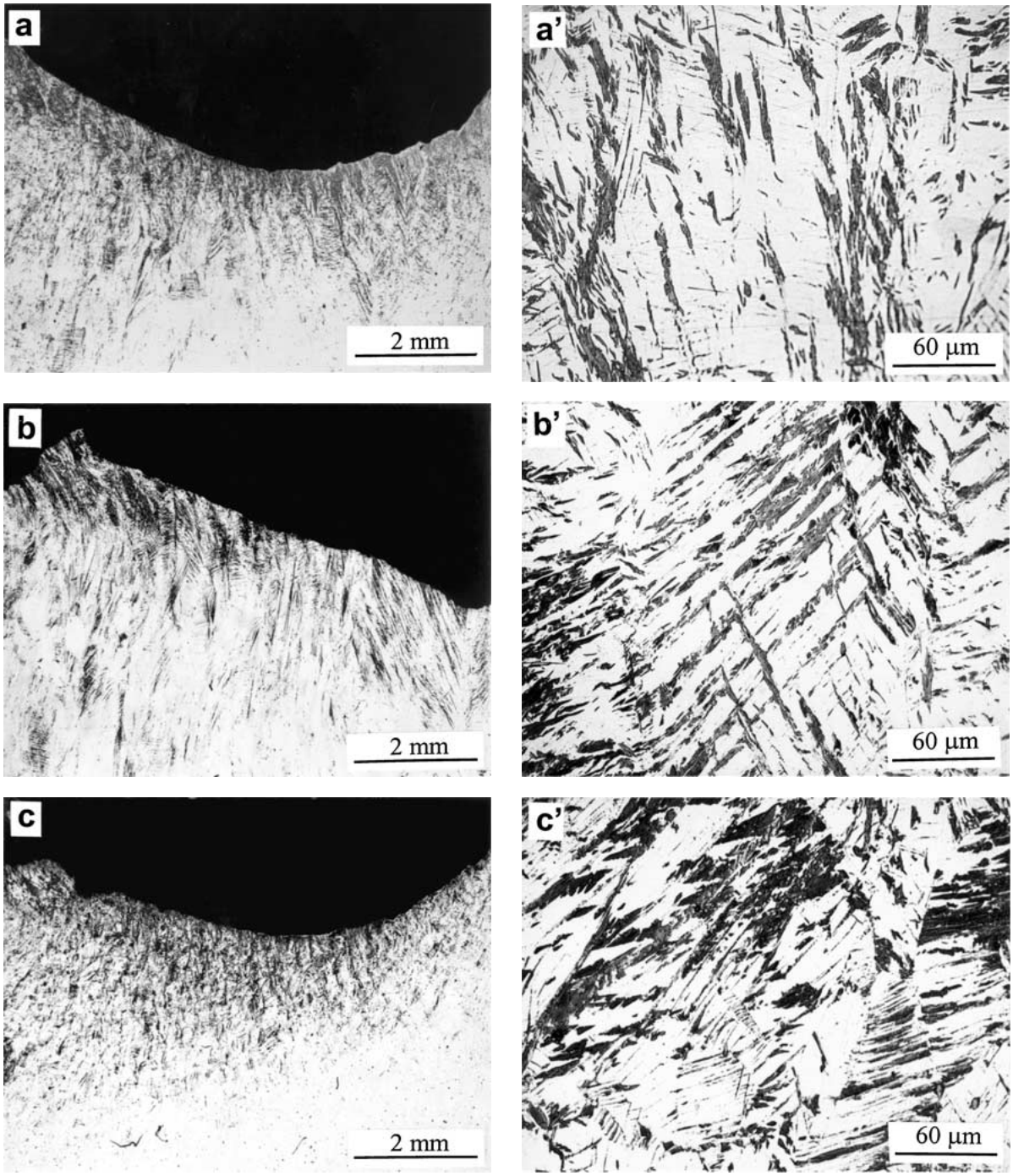

Figure 6 Optical microstructures near the fracture surface of the Charpy specimens tested at different temperature for the dual rolled 2.6Mn alloy. (a, a') 10°C, (b, b') 25°C and (c, c') 50°C.

crack will accelerate the propagation rate of the crack, and leads to a reduction of toughness. At the same time, the formation of martensite at the tip of the advancing crack will absorb energy to complete the transformation. This dissipative process may lead to a net improvement in the toughness [3]. The final change of toughness resulting from the stress-induced martensitic tranformation depends on the balance between the reduction and the improvement. If ΔG is the final change to toughness due to the stress-induced transformation, the energy needed for crack growth in austenite for a given size specimen is G_A, and the energy needed for crack growth in martensite for the same size specimen is G_M, the volume fraction of martensite formed ahead of the crack is V, and the energy dissipated when all the austenite within the martensitic zone transforms to martensite through stress-induced transformation is G_{Asorb}, then:

$$\begin{aligned}\Delta G &= \{VG_{Asorb} + [(1-V)G_A + VG_M]\} - G_A \\ &= VG_{Asorb} + G_A - V(G_A - G_M) - G_A \\ &= VG_{Asorb} - V(G_A - G_M) \\ &= V[G_{Asorb} - (G_A - G_M)] \qquad (1)\end{aligned}$$

In Equation 1 the term within the braces represents the total crack growth energy with stress-induced martensitic transformation, and G_A is the total crack growth energy without stress-induced martensitic transformation. From this equation it can be concluded that:

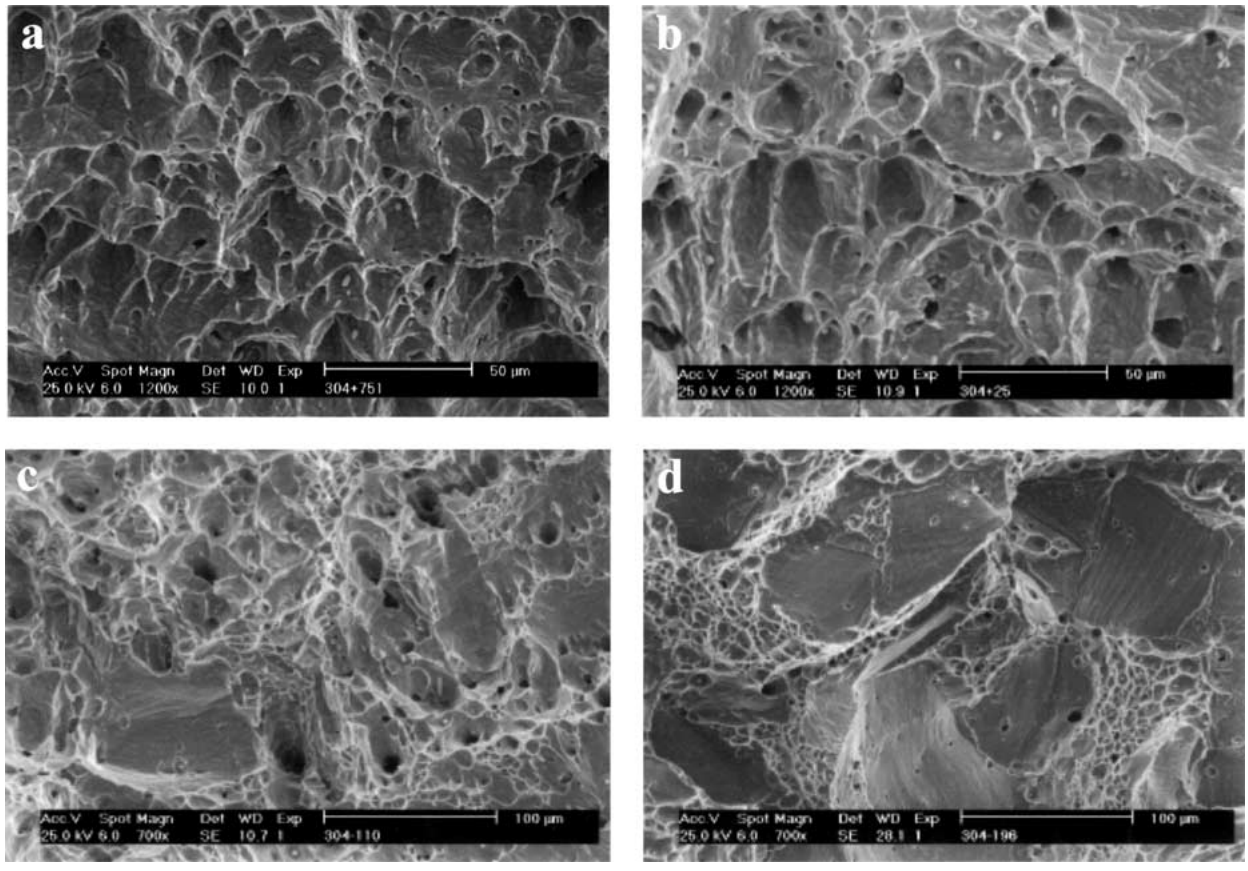

Figure 7 Fracture surface of Charpy specimens of 304 stainless steel impact tested at different temperature. (a) 75°C, (b) 25°C, (c) −110°C and (d) −196°C.

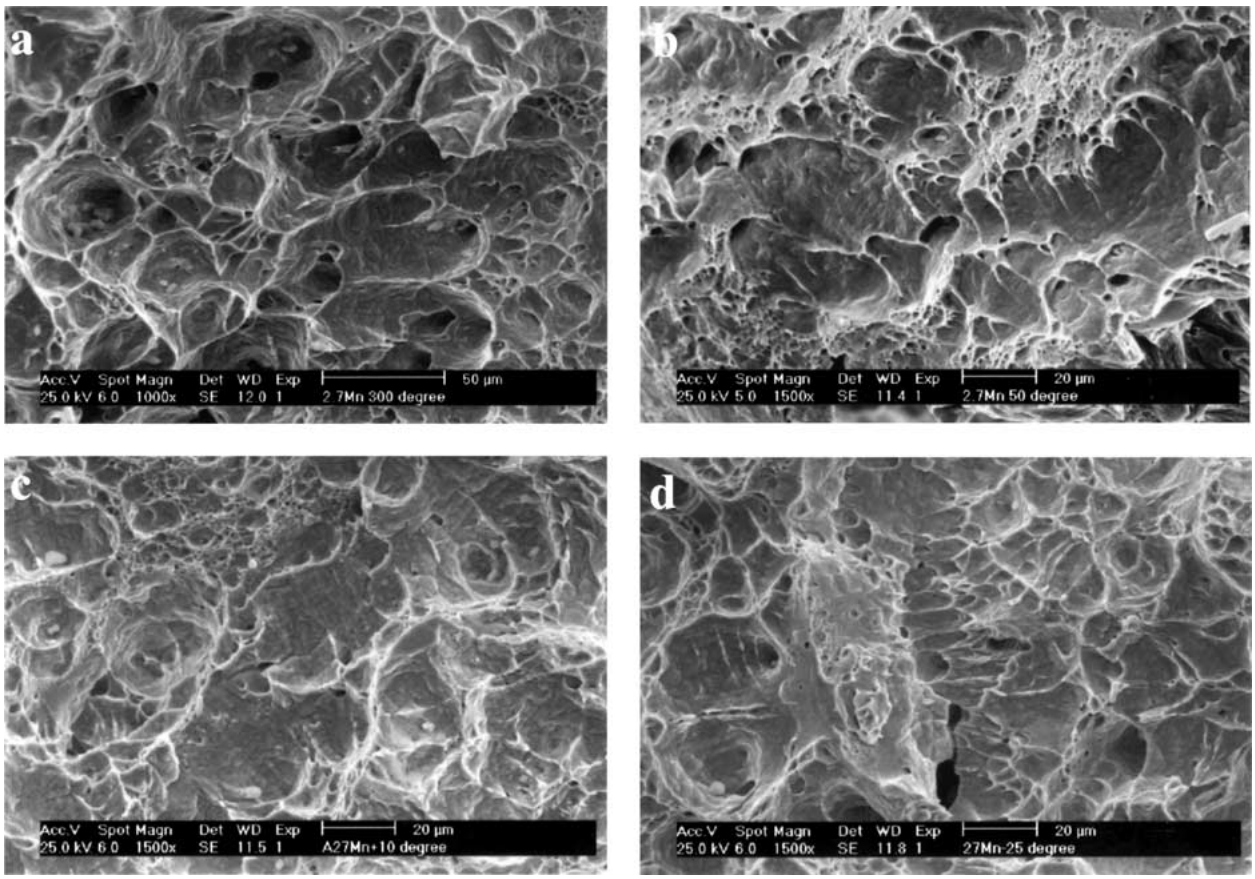

Figure 8 Fracture surface of Charpy specimens of dual rolled 2.6Mn alloy impact tested at different temperature. (a) 300°C, (b) 50°C, (c) 10°C and (d) −25°C.

1. When $\Delta G < 0$, the stress-induced transformation reduces the toughness. When $\Delta G > 0$, it increases the toughness.

2. To ensure positive ΔG, G_{Asorb} must be greater than $(G_{\text{A}} - G_{\text{M}})$. The smaller the difference $(G_{\text{A}} - G_{\text{M}})$, the greater the ΔG can be obtained.

3. The best case is $G_{\text{A}} = G_{\text{M}}$, i.e., the fracture properties of the parent phase and new phase is the same, and all the energy dissipated in the stress-induced transformation is used to improve the toughness of the alloy.

4. The worst case is $G_{\text{M}} = 0$, that is the new phase is extremely brittle. In this case, the bigger the G_{A}, the smaller the ΔG. This implies that for a tough parent phase the stress-induced transformation will make a smaller, possibly negative net contribution to the total toughness.

For very brittle materials, such as ceramics and white cast irons, where G_{A} and G_{M} is very similar, G_{Asorb} is normally greater than $(G_{\text{A}} - G_{\text{M}})$. The stress-induced transformation now makes a positive net contribution to the toughness of material. For plastic materials, such as the austenitic steels used in the present work and many other steels, G_{A} is generally greater than G_{M}. The value of $G_{\text{Asorb}} - (G_{\text{A}} - G_{\text{M}})$ may be positive, negative or zero, depending on the chemical composition of the alloys and the test temperature. For a given alloy, the value of G_{Asorb} is related to the difference between the actual test temperature and the Ms temperature, when the test temperature is between the Ms and Md temperatures. The closer the test temperature to the Ms, the less external energy is required to induce the transformation, therefore, the smaller the work of G_{Asorb}. Since austenite is a FCC phase, its yield stress is not strongly temperature dependent [19] and it is expected that the austenite is still tough even at -196°C [6]. The results in Fig. 3 support this assumption. Thus, for a given alloy, G_{A} can be considered as a constant. G_{M} is very much related to the carbon content of the alloy and the test temperature. For high carbon steels, such as the Fe-Ni-C alloy used in previous work [16], the new phase, martensite is quite brittle, and therefore, G_{M} is very small. But, the parent austenite phase is still very tough and G_{A} is large. Hence, it is quite possible that ΔG is less than 0 ($\Delta G < 0$) in this alloy. This has been confirmed by the previous experimental results and the energy analysis using the crystallographic model for stress-induced martensitic transformation [16]. For low carbon steels, the fracture properties of martensite depend on the temperature. The lower the test temperature, the more brittle the martensite. When the test temperature is above the ITT, the toughness of low carbon martensite is much larger than it is when the test temperature is below the ITT. Hence, the G_{M} value for low carbon martensite at temperatures above ITT is larger than that at temperatures below ITT. It is now possible to obtain a positive ΔG at temperatures above ITT and less likely at temperatures below ITT.

From above analysis it is not difficult to explain the variation of impact energy with the test temperature in Figs 1–3.

304 stainless steel has very stable austenite with an Ms temperature below -196°C. The stress-induced transformation occurs below -25°C under impact conditions. The martensite formed is brittle and the G_{M} is small because of the low test temperature. Hence, as the test temperature decreases, the amount of the brittle stress-induced martensite is increased, and the toughness decreases as shown in Fig. 1. At test temperature above 0°C, no stress-induced martensitic transformation occurred. The slightly increase of impact energy from 0°C to 150°C may be associated with the removal of residual stress at the root of the notch caused by the notch grinding. The lower impact energy at 250°C is still not fully understood.

The stress-induced transformation in 2.6Mn alloy occurs at higher temperatures. The highest temperature, at which the stress-induced transformation may occur, is 170°C for solution treated 2.6Mn alloy and 50°C for the dual rolled 2.6Mn alloy. Therefore, the martensite formed is more ductile and has a higher G_{M} than it is at low test temperatures, particularly when the test temperature is above the its ITT. Hence, the stress-induced transformation may lead to net toughening, i.e., a positive ΔG. For the impact test results of the solution treated 2.6Mn alloy in Fig. 2a, within the temperature range between 100°C and 170°C, stress-induced martensite formed under impact conditions and as the test temperature decreased the amount of martensite formed increases. This results in the significant improvement of the toughness within this temperature range. When the temperature is below 80°C, athermal martensite formed prior to testing, and the amount of the athermal martensite increases as the test temperature decreases. Hence, the impact energy falls dramatically as the test temperature decreases. In Fig. 2a, when the test temperature is over 170°C, the impact energy shows no significant change. This is due to the inactivity of impact energy of austenite to the test temperature as shown in Fig. 3. The reasons for the independence of impact toughness of pure austenite on the test temperature may be associated with its FCC structure, in which the sliding systems are much more than other structures of metals. The same explanation can be applied to Fig. 2b. In this figure the temperature range for transformation toughening is shifted to a lower temperature between 10°C and 50°C.

In 1969 Gerberich *et al.* [2] studied the effect of the stress-induced martensitic transformation on the plastic energy dissipation and indicated that the energy dissipated by transformation may be about 5 times higher than the plastic dissipation processes normally occurring at a crack tip within either austenite or martensite or the mixture of both. The present authors consider that although the energy dissipated by the martensitic transformation is large, the energy required to induce the transformation does not come solely from the interaction with the external stress. Most of the energy required for the transformation comes form the thermodynamic free energy difference between austenite and martensite $\Delta G_{\gamma \to \alpha}$, and this increases as the temperature decreases. In fact, the stress-induced transformation will not occur if the value of $\Delta G_{\gamma \to \alpha}$ is less than the value of thermodynamic free energy change at

the Md temperature. In terms of transformation within a unit volume of material, let G_{IS} represent the energy required for the transformation, and G_{ex} denote the energy provided by the external stress inducing the transformation. Then, G_{ex} is the only energy term that may contribute to the toughness, and the G_{Asorb} in Equation 1 can be represented by:

$$G_{Asorb} = V_M \cdot G_{ex} \tag{2}$$

where V_M is the volume of the martensitic zone. It follows, that,

$$G_{IS} = \Delta G_{\gamma\to\alpha} + G_{ex} \tag{3}$$

At and below the Ms temperature $\Delta G_{\gamma\to\alpha} \geq G_{IS}$, and external energy is not required for the transformation. Above Md temperature, stress-induced martensite can not form. When the temperature is between Ms and Md, the occurrence of stress-induced transformation requires the assistance provided by the external energy G_{ex}. As the temperature approaches to the Ms temperature, $\Delta G_{\gamma\to\alpha}$ increases and the required external energy G_{ex} decreases. But, at the same time the total amount of martensite formed increases, thus, the size of the martensitic zone V_M and/or the volume fraction of martensite within this zone V increases. This means that the total G_{Asorb} does not significantly decreases, and may even increase.

From this analysis we can understand that even though the energy dissipated by the transformation is up to 5 times higher than the normal plastic dissipation processes [2], the stress-induced transformation still decreases the impact toughness in some alloys, such as high carbon Fe-Ni-C alloy and 304 stainless steel. Otherwise, the transformation in any alloy should dramatically change the toughness.

4.2. Calculation of the dissipated energy in the dual rolled 2.6Mn alloy

The crystallographic model for stress-induced martensitic transformation, which was originally developed for ceramic materials [20–22] and later successfully extended to a high carbon Fe-Ni-C alloy [23, 24], has been employed for the present low carbon austenitic steel. The analysis in the previous paper [16] and Equation 6 to 13 in this reference have been used to calculate the impact energy of the dual rolled 2.6Mn alloy. Because of the difficulty of obtaining full martensite in 304 stainless steel (its Ms temperature is below -196°C) and the influence of the ε martensite, it is difficult to apply this crystallographic model to this steel. Thus, the calculation of impact energy was carried out only on the dual rolled 2.6Mn alloy, where the Ms temperature is just below room temperature.

The most difficult part of the application of the crystallographic model to low carbon steels is to estimate the shape strain matrices for lath martensite using the phenomenological theory [25], which is able to predict the habit planes, orientation relationship, the shape strain and the internal substructure from the first principle input of the lattice parameters of austenite and martensite and the lattice invariant shear system. Unlike plate martensite in high carbon steels, lath martensite in low carbon steels normally shows no signs of internal twinning, and instead has a substructure consisting of a dense tangle of dislocations. The habit plane determined for lath martensite also differs from that of plate martensite [26]. Following Ross and Crocker [27], Kelly [26] has used the double lattice invariant shear formulation to calculate the crystallographic features of the martensitic transformation in low carbon steels. The process is very complex and the results show considerable scatter. Fortunately, Wakasa and Wayman [28–30] have studied the same alloy in much detail and provided crystallographic information needed for the present study. Hence, it is possible to simplify the process. As an approximation, a single lattice invariant shear with the shear system of $\{112\}_A\ \langle 110\rangle_A$ was used to calculate the shape strain matrices using the phenomonological theory. The lattice parameters of austenite and martensite were determined by X-ray diffraction, to be 0.35835 nm for austenite and 0.28742 nm for martensite. Because of the low carbon content, the martensite can be considered as cubic [31]. The calculated results are as follows: The magnitude of the shape strain is 0.351562, which is very close to the experimentally determined value of 0.31–0.33 [30]. The predicted orientation relationship between parent austenite and martensite agrees very well with the Kurdjumov-Sachs relationship, which is the dominant orientation relationship in the low carbon Fe-Ni-Mn-C alloy [29]. The predicted habit is $\{0.358012, -0.741735, 0.567147\}_A$, which is 15.8° away from $\{111\}_A$. The habit plane determined by Wakasa and Wayman [28, 29] ranged from 4.5° to 8.0° from $\{111\}_A$. Hence, as an approximation, the crystallographic features predicated by the phenomenological theory with single shear are acceptable.

All the other analysis procedures for calculating the impact energy using the crystallographic theory for stress-induced martensitic transformation in low carbon steels is exactly the same as that in Ref [16] for high carbon steel. The fracture strength of martensite was measured from tensile tests of specimens that had been quenched in liquid nitrogen. The fracture strength of austenite was measured using the 5.8Mn alloy, which does not transform in tension at room temperature. As the temperature range from 10°C to 50°C is so small, the fracture strength at room temperature is employed over this range. The work done by the external stress in inducing the transformation, U_{WORK}, was calculated using Equation 11 in Ref. [16]: i.e.,

$$U_{WORK} = V_{M\text{-}ZONE} \cdot \sum U^i_{WORK}$$
$$V^f_M = \sum V_i \tag{4}$$

where U^i_{WORK} is the work required to induce transformation in individual grains, $V_{M\text{-}ZONE}$ is the volume of the martensitic zone near the fracture surface in the Charpy specimens, V^f_M is the average volume fracture of martensite within the martensitic zone, and V_i is the contribution of each transformed grain makes to the final average volume fraction of martensite V^f_M.

TABLE II The calculated experimental data in the analysis of Charpy impact toughness at 10°C, 25°C and 50°C using the crystallographic model for transformation toughening in dual rolled 2.6Mn alloy

Temp (°C)	$V_{\text{M-ZONE}}$ (10^{-6} m^3)	V_M^f (%)	V_M^{tip} (%)	σ_f^A (MPa)	σ_f^M (MPa)	σ_f (MPa)	U_{WORK} (*J*)	U_0^A (J)	U_g^M (J)	U_g^A (J)	A_K^{cal} (*J*)	A_K^{Exp} (J)
10	0.6666	32	42	1153	1430	1269	*52.1*	44	39.	91	*165.3*	173
25	0.5333	27	38	1153	1430	1258	*39.0*	44	42	91	*155.4*	163
50	0.4395	19	39	1153	1430	1261	*21.7*	44	44	91	*138.4*	141

A_K^{cal} and A_K^{Exp} are the calculated and experimental A_K value, respectively.
Italic indicates that the data in the column is calculated. All other data is measured.

The energy for crack growth in martensite, U_g^M, was measured using the pre-cracked Charpy specimens with a crack depth of 2 mm tested at different temperatures. These Charpy specimens were quenched in liquid nitrogen, so that almost full martensite was obtained. The energy for crack growth in austenite, U_g^A was measured using the same pre-cracked specimens that was as dual rolled, and tested at 120°C, where no transformation occured. The energy for crack formation in austenite is the difference between the impact energy of the normal Charpy specimens and the pre-racked specimens. Thus, the total impact energy A_K^{Cal} can be calculated using the Equation 13 of Ref. [16]:

$$A_K = U_0^A + U_{WORK} + \left[U_g^M \cdot V_M^{tip} + U_g^A \cdot \left(1 - V_M^{tip}\right)\right] \quad (5)$$

where V_M^{tip} is the average volume fracture of martensite along the whole crack.

The final calculated results of the impact energy for the dual rolled 2.6Mn alloy, together with the experimental result, are listed in Table II. In the table, σ_f represents the overall fracture strength of the material ahead of the tip of the crack. It can be calculated from the Equation 12 of Ref. [16] i.e.,

$$\sigma_f = V_M^{tip}\sigma_f^M + \left(1 - V_M^{tip}\right)\sigma_f^A \quad (6)$$

where V_M^{tip} is the volume fraction of martensite in the region of ahead of the crack tip.

From the results of Table II, it can be seen that the increase of impact toughness of the dual rolled 2.6Mn alloy, as the test temperature is lowered from 50°C to 10°C, is the result of the increase in the energy dissipated during the transformation. This increase in the energy dissipated is due to the increase in the martensitic zone size near the fracture surface in the Charpy specimens, and therefore, the increase in the total amount of martensite formed by the stress-induced transformation. The energies of crack formation and crack growth are relatively independent of temperature within the range 50°C to 10°C.

5. Conclusions

1. In the commercial 304 stainless steel, stress-induced martensitic transformation occurs at test temperatures below −25°C under impact conditions, and leads to the formation of both ε and α martensite. This transformation makes a negative net contribution to the overall impact toughness because of the low toughness of the α martensite formed at low temperatures. As the test temperature drops, the impact toughness decreases.

2. In the low carbon 2.6Mn alloy, the stress-induced martensitic transformation, under Charpy impact conditions, occurs at temperatures below 170°C and 50°C for the solution treatment and the dual rolled conditions, respectively. In both cases the transformation makes a positive net contribution to the impact toughness because of the high toughness of the martensite at these high temperatures. The toughness of the alloy increases with decreasing test temperature up to the point where athermal martensite is formed.

3. The present results strongly support the early conclusion [1] that the magnitude of the toughness change depends on the balance between the fracture properties of the new phase and the energy dissipated at the tip of crack. Much previous work reported only positive net changes in fracture toughness. The present work provides an example of a negative net change in impact toughness as a result of stress-induced transformation.

4. A recently developed crystallographic model for the stress-induced martensitic transformation has been successfully used to analyse the effect of the transformation on the impact toughness in the dual rolled 2.6Mn alloy. The toughness calculated using this model agrees well with the experimental results. From the calculated data it can be seen that the increase of impact toughness of the dual rolled 2.6Mn alloy with the test temperature decrease from 50°C to 10°C results from an increase in the energy dissipated by the transformation. This is due to the increase in the martensitic transformation zone near the fracture surface in the Charpy specimens, and the consequential increase in the total amount of martensite formed by the stress-induced transformation.

Acknowledgement

The work in this paper was supported by an Australian Research Council (ARC) Large Grant. The authors are most grateful for this support.

References

1. A. G. MAMALIS and G. N. HAIDEMENOPOULOS, *J. Mater. Proc. Tech.* **30** (1992) 211.
2. W. W. GERBERICH, P. L. HEMMINGS, V. F. ZACKAY and E. R. PARKER, in "Fracture" (Chapman & Hall, London, 1969) p. 288.
3. S. D. ANTOLOVICH, *Trans. TMS-AIME* **242** (1968) 2371.
4. S. D. ANTOLOVICH and B. SINGH, *Metall. Trans.* A **1** (1970) 3463.
5. *Idem., ibid.* **2** (1971) 2135.
6. S. D. ANTOLOVICH, *Engineering Fracture Mechanics* **4** (1972) 133.

7. V. F. ZACKAY, E. R. PARKER, D. FAHR and R. BUSCH, *Trans. ASM* **60** (1967) 252.
8. W. W. GERBERICH, P. L. HEMMINGS, M. D. MERZ and V. F. ZACKAY, *ibid*. **61** (1967) 843.
9. W. W. GERBERICH, P. L. HEMMINGS and V. F. ZACKAY, *Metall. Trans*. A **2** (1971) 2243.
10. S. K. HANN and J. D. GATES, *J. Mater. Sci*. **32** (1997) 1249.
11. F. F. LANGE, *ibid.* **17** (1982) 225.
12. A. G. EVANS and R. M. CANNON, *Acta Metall*. **34** (1986) 761.
13. D. M. STUMP, *Phil. Mag*. **64** (1991) 879.
14. D. M. STUMP and R. A. LA VIOLETTE, *ibid*. **68** (1993) 35.
15. Q. P. SUN, K. C. HWANG and S. W. YU, *J. Mech. Phys. Solids*. **39** (1991) 507.
16. M-X. ZHANG and P. M. KELLY, *Metall. Mater. Trans*. **32A** (2001) 2695.
17. J. A. VENABLES, *Phil. Mag*. **7** (1962) 35.
18. P. M. KELLY, *Acta Metall*. **13** (1965) 635.
19. D. MCLEAN, in "Mechanical Properties of Matter" (John Wiley, New York, 1962) p. 97.
20. C. J. WAUCHOPE and P. M. KELLY, *J. Amer. Ceram. Soc*. **78** (1995) 2853.
21. *Idem*., *Key Eng. Mater*. **153/154** (1998) 125.
22. P. M. KELLY and L. R. F. ROSE, *Progress in Materials Science*, in press.
23. M.-X. ZHANG, P. M. KELLY and J. D. GATES, *Mater. Sci. Eng*. A **273–275** (1999) 251.
24. *Idem*., in Proceedings of the International Conference on Solid-Solid Phase Transformations'99, Kyoto, May 1999, edited by M. Koiwa, K. Otsuka and T. Miyazaki (The Japan Institute of Metals, Japan, 1999) p. 1032.
25. J. S. BOWLES and J. K. MACKENIZE, *Acta Metall*. **2** (1954) 129.
26. P. M. KELLY, *Mater. Trans. JIM* **33** (1992) 23.
27. N. H. D. ROSS and A. G. CROCKER, *Acta Metall*. **18** (1970) 405.
28. K. WAKASA and C. M. WAYMAN, *Ibid*. **29** (1981) 973.
29. *Idem*., *ibid*. **29** (1981) 991.
30. *Idem*., *ibid*. **29** (1981) 1013.
31. G. V. KURDJUMOV, *J. Iron Steel Inst*. **180** (1960) 26.

Received 22 October 2001
and accepted 6 May 2002